Heliyon 10 (2024) e36165

Contents lists available at ScienceDirect

Heliyon

journal homepage: www.cell.com/heliyon

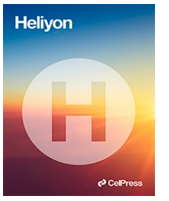

Research article

Aluminum-induced oxidative stress promotes changes in the structure of the gut microbiota and liver deficiency

Rong Feng [a,*], Liang Chen [b], Ming Yang [b]

[a] Chongqing City Vocational College, Yongchuan, Chongqing Municipality, China
[b] School of Life Sciences, Jiangsu University, Zhenjiang, Jiangsu province, China

ARTICLE INFO

Keywords:
Aluminum
Gut microbiota
Oxidative stress
Gut-liver axis
Inflammation

ABSTRACT

As a low-toxicity metal, aluminum has garnered increasing attention in relation to its impact on the human body; however, the specific mechanism of action remains unclear. To bridge this knowledge gap and facilitate practical applications, this study took 8-week-old ICR mice as the research object to study the effects of dietary addition of aluminum potassium sulfate on intestinal flora structure and liver. As the concentration of aluminum increased, it inhibited mice weight growth rate and significantly altered the composition of white blood cells in their bloodstream. Histological examination revealed liver inflammation through HE staining sections. The oxidative stress markers MDA increased, GSH-PX and CAT decreased significantly. And liver function index MAO increased, TC and ALP decreased first and then increased. Moreover, there was a significant increase in pro-inflammatory factor TNF-α content. Further 16S rRNA sequencing analysis demonstrated substantial changes in both composition and structure of mouse intestinal microbiota induced by aluminum exposure; microbial phenotype prediction indicated that aluminum-induced oxidative stress promoted an increase in abundance of oxidation-resistant microbial types. Alterations in gut flora structure also influenced the liver via the gut-liver axis. These findings lay a foundation for further research on the regulation and interaction of aluminum on intestinal flora.

1. Introduction

Aluminum, a naturally abundant metallic element, has found extensive applications across various fields since its discovery, including as food additives and pharmaceutical adjuvants. In terms of food additives, aluminum-containing compounds can be incorporated into food as leavening agents, stabilizers, and colorants. Due to its non-essential nature in the human body, the toxicity of aluminum to organisms has garnered increasing attention. Regarding its impact on the liver, which serves as the primary metabolic organ in humans, it is highly susceptible to harmful metabolites generated during metabolism. Previous studies have demonstrated that aluminum-induced hepatotoxicity is characterized by elevated serum aspartate transaminase, alkaline phosphatase and alanine aminotransferase activities. Serum aminotransferases serve as indicators of liver injury and are released from damaged liver cells into plasma following hepatocyte degeneration or changes in liver membrane permeability. This was further confirmed through liver histopathology analysis revealing hepatocyte congestion and diffuse degeneration accompanied by sinus artery dilation [1–3]. Additionally, liver metastasis occurred after in situ injection of $AlCl_3$ transformed cells into mice [4]. Mechanistic explorations at both

* Corresponding author. Chongqing City Vocational College, Yongchuan, Chongqing Municipality, China.
E-mail address: fr131@163.com (R. Feng).

https://doi.org/10.1016/j.heliyon.2024.e36165
Received 16 February 2024; Received in revised form 9 August 2024; Accepted 12 August 2024
Available online 13 August 2024

cellular level in vitro and investigations on nervous system disorders, hepatic diseases and other tissue-related ailments in vivo mammals have been extensively conducted.

Aluminum potassium sulfate (APS) is a double salt composed of potassium sulfate and aluminum sulfate with crystal water content. Its chemical formula is KAl(SO4)2·12H2O; it exists as colorless cubic monoclinic or hexagonal crystals. Within the food industry, in China, especially in the northern regions, APS has traditionally been added to fried dough sticks since ancient times for its ability to generate carbon dioxide gas through chemical reactions with baking soda thereby creating a porous structure within the dough resulting in fluffy and crispy dough sticks. The use of APS as an aluminum carrier has received limited research attention thus far compared to predominantly using aluminum trichloride for research. In the field of Chinese cuisine, APS is legally permitted for use [5]. Therefore, to provide a more precise elucidation of aluminum absorption and its impact, this study focuses on APS as the representative form of aluminum.

The gut microbiota plays a crucial role in numerous physiological functions within the human body and is even regarded as an essential 'organ' safeguarding human health. As venous blood from the gut reaches the liver first, it becomes susceptible to microbial metabolites absorbed through contact with gut microbiota or via translocation across the intestinal epithelial barrier [6]. Dysregulation of gut microbiota including disruption of gut barrier integrity, microbial translocation into systemic circulation, and inflammatory immune responses induced by lipopolysaccharides (LPS) are closely linked to cirrhosis pathogenesis and hepatocellular carcinoma development [7]. On the other hand, the liver also regulates the gut microbiota through the liver-gut axis, and bioactive substances such as bile acids synthesized by the liver can also be secreted to the intestine for metabolism, thus inhibiting the overgrowth of intestinal bacteria. Due to their common embryonic origin, the liver and intestine are closely related in terms of anatomy and biological function. They communicate bidirectional through bile duct, portal vein and systemic circulation [8]. This study aims to explore how oral administration of aluminum-containing food additives affects the structure of gut microbiota while investigating the intricate relationship among aluminum exposure and liver function.

2. Materials and methods

2.1. Animal

Thirty 8-week-old male ICR mice were purchased from Beijing Vital River Laboratory Animal Technology Co., LTD. All animal experiments were approved by Jiangsu University Institutional Animal Care and Use Committee (UJS-IACUC-2020051201) and followed the guidance and regulations of the National Institutes of Health Experimental Animal Care and Use Guidelines.

Thirty mice were randomly divided into three groups with 10 mice in each group. They were divided into high-dose aluminum group (HA group, adding 50 g/kg APS in the standard feed), low-dose aluminum group (LA group, adding 20 g/kg APS in the standard feed) and control group (CON group). By referring to relevant literature and preliminary experiments, we chose 20 g/kg and 50 g/kg as the low and high doses. Except for the added APS components, the food components of the treated and control groups were the same. Continuous feeding for 120 days, without using utensils containing aluminum products. All mice were placed in a controlled environment of 20 °C–26 °C, 40%–70 % humidity, and a light-dark cycle of 12 h.

2.2. Body weight

The mice were weighed on the first day of feeding, and then weighed every 30 days, and the feeding cycle was 120 days. A total of 5 times were weighed. Each mouse was labeled, and the weight data of each mouse was recorded and counted. Calculate the growth rate for each month, growth rate = (weight this month - weight last month)/weight last month × 100 %. Statistical analysis and mapping were performed using Prism 5 software.

2.3. Blood routine examination

Intravenous blood collection was performed on the mice on the 60th and 120th day respectively. For the first time, blood collection was performed via posterior eyeball veins. Capillaries were placed at the inner corner of the eye and pierced at a 45-degree Angle with the mouse's face, then slid to the back of the eyeball and gently pierced into the fundus. For the second time, the eyeball was removed and blood was taken before the death. The eye skin was lightly pressed to make the eyeball protrude. The eyeball was quickly extracted with ophthalmic bending forceps, and the blood was connected to the anticoagulant tube. 20 μl whole blood was inserted into the sample needle of the automatic blood cell analyzer (BC2800Vet, Shenzhen Miray Biology) for routine blood analysis. The main parameters were: neutrophil percentage (Gran%), lymphocyte percentage (Lymph%), monocyte percentage (Mon%).

2.4. Histological observation

The mice were killed by cervical dislocation and liver tissue was collected. After being fixed in a refrigerator at 4 °C for 8–12h with 4 % PFA, it was placed in 30 % sucrose solution. After the tissue sank to the bottom, it was removed, washed with PBS, filtered by filter paper, buried in a paper box equipped with OCT, and put into a −80 °C refrigerator for rapid freezing. Slices were cut into 30 μm slices with a frozen microtome and stained successively with hematoxylin-eosin (H&E) solution. The sections were sealed with neutral glue and observed under optical microscope.

2.5. Oxidative stress and liver function index detection

The dissected liver is washed in normal saline, then drained with filter paper, and then small pieces of tissue are cut and weighed. PBS (ml, 0.01M, pH 7.4) at 2–8 °C was added at a ratio of 9 times tissue weight (g) for homogenization. The homogenization was done on ice. After centrifugation at 4 °C, 10,000×*g* for 10 min, the supernatant was taken and placed on the ice to be measured.

The content of Malondialdehyde (MDA) and Reduced glutathione (GSH) and the activity of Glutathione Peroxidase (GSH-PX), Superoxide dismutase (SOD) and Catalase (CAT) were strictly operated according to the instructions of MDA colorimetric test kit (TBA method), GSH colorimetric test kit, GSH-Px test kit, Total superoxide dismutase (T-SOD) colorimetric test kit and CAT colorimetric test kit respectively. The protein content of liver tissue homogenate was determined according to the instructions of BCA kit. The above kit manufacturers are Elabscience, the origin is Wuhan, China.

The same method was used to homogenize the tissue with PBS, and the LDH and ALP indexes were detected after centrifugation. Isopropyl alcohol should be used to homogenize tissue samples for TC index detection. The tissue used for Monoamine oxidase (MAO) testing is homogenized according to the kit instructions. The above indexes were detected by LDH colorimetric test kit, ALP colorimetric test kit, TC colorimetric test kit and MAO colorimetric test kit respectively. The above kit manufacturers are Elabscience, the origin is Wuhan, China.

2.6. TNF-α and IL-1β detection

The contents of Tumor necrosis factor (TNF-α) and Interleukin 1 beta (IL-1β) were determined by ELISA and strictly followed the instructions of the Mouse TNF-α ELISA kit and Mouse IL-1β ELISA kit (ELK Biotechnology, Wuhan, China).

2.7. Fecal sample collection, DNA extraction and sequencing

During the same time period after feeding, 10 mice from each group were placed in 10 alcohol-cleaned cages. One stool was collected from each mouse, placed in a EP tube, and collected 3 times for 3 repeated tests. And then placed in liquid nitrogen for rapid freezing, and stored in the laboratory refrigerator at −80 °C. The genomic DNA of the samples was extracted using the E.Z.N.A. Stool DNA separation kit (Omega Bio-tek, United States), and the concentration and purity of genomic DNA were detected by UV–visible spectrophotometer and 1 % agar-gel electrophoresis. Use a universal primer upstream with Barcode sequence (5 ′-ACTCCTACGG-GAGGCAGCA-3′, 338F; 5 ′-GGACTACHVGGGTWTCTAAT-3′, 806R) to amplify the V3–V4 variable region of the 16S rRNA gene. Shanghai Majorbio Bio-Pharm Technology Co., Ltd. performed library construction, sequencing and subsequent data. The original data of 16S sequencing in this study have been uploaded to the online repository NCBI for Submission ID: SUB11009633, 11062312, BioProject ID: PRJNA804675, 805,015.

2.8. Bioinformatics data analysis

The Uparse(version 7.0.1090 http://drive5.com/uparse/)software was used to cluster the high-quality sequences obtained after demultiplexing, filtering, merging and dehybridization optimization of the original sequences of 16S rRNA genes into operational classification units (OTUs). The classification of each OTU represented sequences was analyzed by RDP classifier(version 2.11) Bayesian algorithm, and the annotation results with confidence threshold above 0.7 were retained. The composition and abundance of each sample were counted at each classification level, and R software was used for visualization analysis. The linear discriminant analysis effect size (LEfSe) algorithm was used to identify the difference of different groups. The Kruskal-Wallis H test was used to identify the phyla and genera with significant abundance differences within the taxa. The biomarkers of LEfSe analysis performed in microbiome studies had an effect size threshold of 2, identifying flora with significant differences in abundance between groups (from phylum to genus).

PICRUSt is a software package for functional prediction of 16S amplicon sequencing results. First, the OUT-abundance table was standardized by PICRUSt to remove the influence of the copy number of 16S maker gene in the species genome, and then the greengene id corresponding to each OUT was compared to the Kyoto Encyclopedia of Genes and Genomes (KEEG) database. Information on the three levels of the KEEG Pathway can be obtained, and the abundance of each horizontal pathway can be obtained and visualized as bar charts and heat maps.

BugBase is an online microbiome analysis tool that identifies high levels of phenotype present in microbiome samples, enabling phenotypic prediction. BugBase first normalizes the OTU with the predicted 16S copy number and then predicts the microbial phenotype using the pre-calculated file provided.

2.9. Statistical analysis

The SPSS 17.0 software and Graphpad Prism software were used for statistical analysis. Dates in figures were presented as means ± S.E.M,n = 3 or 10, as described in the diagram. One-way ANOVA and Kruskal-Wallis H test were used to analyze the significant differences in the abundance of two groups and multiple groups of microbial communities and metabolites, respectively. FDR was used to correct P values for multiple tests. Corrected P values < 0.05 were considered significant difference. Other statistical analysis methods are described in detail.

3. Results and discussion

3.1. Growth rate of body mass

Since the initial weight of each mouse is different, the growth rate method was used to explore the effect of different doses of aluminum on the weight of mice. As can be seen from Fig. 1A, the growth rate of all groups was higher at 30 days, and the control group had a relatively higher growth rate than the treatment group, while the growth rate of the low dose (LA) and high dose (HA) groups had no significant difference compared with the control group ($P > 0.05$). After 60 days, the growth rate of the control group decreased slightly, while the growth rate of the treatment group decreased significantly. Compared with the control group, the growth rate of LA was significantly different ($P < 0.01$), and the growth rate of HA was significantly different ($P < 0.001$). At 90 days, the growth rate of body weight tended to be stable. Although the growth rate of LA group was higher than that of other groups, there was no significant difference among all groups ($P > 0.05$), which was not statistically significant. At 120 days, the growth rate of all groups decreased significantly, and the decline was more obvious in the treatment group. At 120 days, compared with the control group, there was no significant difference in the growth rate of the LA group ($P > 0.05$), but there was a significant difference in the HA group ($P < 0.05$). Aluminum is a chronically toxic element, and it is newly exposed to aluminum at the first 30 days. At this stage, the influence on host is relatively small, and there is no significant difference in body weight growth rate among all groups. At the second 30 days, it can be seen that different doses of aluminum have different effects, and low to high doses of aluminum-containing diet lead to a significantly reduced trend of body weight growth, indicating that it is related to the concentration of aluminum exposure. At the third 30 days, the growth of mice reached the peak, the weight growth was gentle, and the growth rate of control group was not different from that of each group. At the fourth 30 days, when the growth and metabolism rate of mice decreased, the growth rate of each group further decreased, and the HA group also showed a significantly reduced growth rate, which also indicated the correlation between the growth rate and the aluminum concentration gradient. In conclusion, aluminum significantly inhibited the rate of weight gain in mice. Similar results were obtained by Cheng et al. [9] and Abdel-Aal et al. [10].

3.2. Effect on blood routine indexes of mice

As can be seen from Fig. 1D, the proportion of neutral cells in the treatment group was significantly increased over time, especially in the HA group ($P < 0.01$), while there was no significant change in the control group. The white blood cells in the blood are mainly composed of neutrophils, lymphocytes and monocytes. Neutrophils are the immune vanguard, accounting for a relatively low proportion in the body under normal conditions. They are quickly recruited and aggregated when inflammation occurs, accounting for up

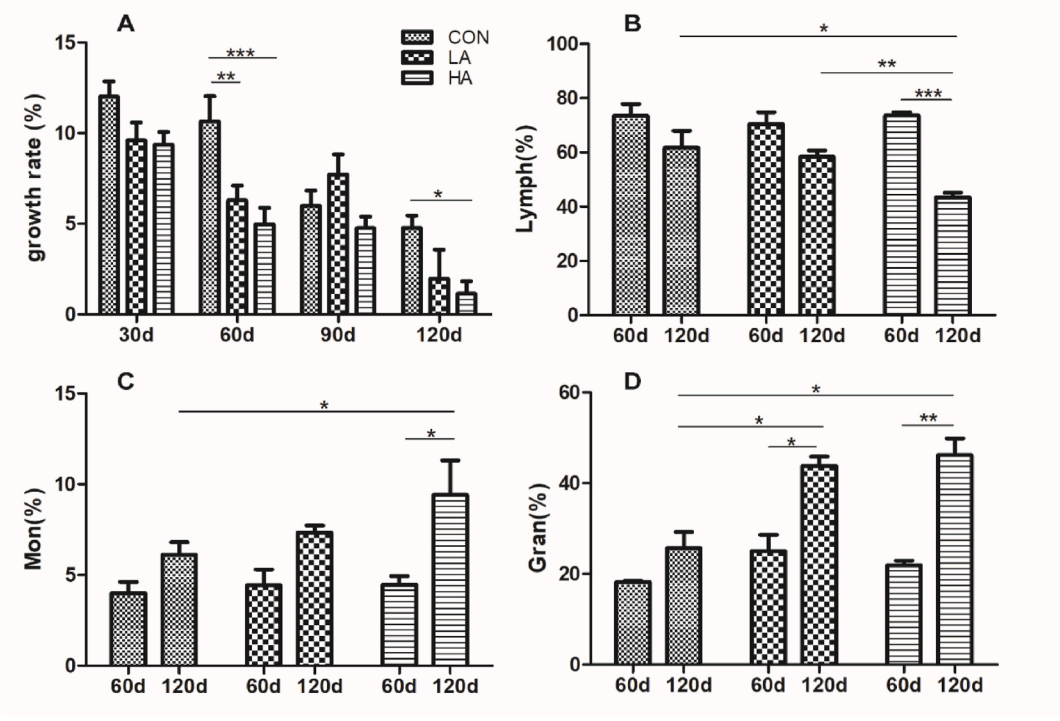

Fig. 1. A: Change in growth rate. The error bars indicate S. E. M. n = 3.
B-D: Changes in the composition of white blood cells in the blood. B: Percentage of lymphocytes; C: Percentage of monocyte; D: Percentage of neutrophils. The error bars indicate S. E. M. n = 3. $^{*}P < 0.05$, $^{**}P < 0.01$, $^{***}P < 0.001$.

to 70 % of white blood cells. They play a very important role in specific cellular immunity in the blood and have strong chemotactic, phagocytic and bactericidal effects, so they are commonly used as an evaluation indicator of inflammation [11]. Neutrophils are highly pro-inflammatory. Therefore, prolonged activation and excessive accumulation of neutrophils can lead to tissue damage and chronic inflammation [12]. An important activity of neutrophils is the release of reactive oxygen species (ROS). During an oxidative burst, neutrophils consume oxygen, converting it into superoxide radicals via the NADPH oxidase 2 (NOX2) complex [13,14]. Some of these free radicals may covalentially bind to macromolecular structural proteins or PUFA in liver cell biofilms such as mitochondria and microsomes, reducing liver glutathione content and glutathione S-transferase and catalase activity [15,16]. In the liver, neutrophils promote the metastasis cascade by forming neutrophilic extracellular traps (NETs), which play an important role in promoting tissue damage and tumor progression [17].

As can be seen from Fig. 1B there was little change in the proportion of lymphocytes in the control group and the low-dose group, while there was a significant reduction in the high-dose group ($P < 0.001$).

Lymphocytes are the smallest types of white blood cells. The low percentage of lymphocytes may be caused by the body's inflammatory response and the relatively high percentage of neutral cells. Because lymphocytes are an important force in the body's immune response, when the body's immune function declines, the percentage of lymphocytes will also decrease. Aluminum can induce micronucleus and apoptosis of lymphocytes [18]. Further studies have found that aluminum may lead to genotoxicity of hemocyte through oxidative damage, including increased micronucleus and chromosomal aberrations, and positive results of comet experiments [19,20].

As can be seen from Fig. 1C, the proportion of monocytes in the high-dose group changed significantly ($P < 0.05$), while there was no significant change in the control group and low-dose group. Monocytes are produced in the bone marrow, then enter the blood, and further mature into macrophages, which are the largest cells in the body, and their main function is to produce immunity by phagocytosis and cleaning up foreign invasive organisms. Therefore, an elevated monocyte ratio is also commonly associated with inflammation. Vaccine adjuvants usually contain aluminum, which can significantly up-regulate the secretion of IL-1β and IL-6, and then play a mild role in activating monocytes to participate in innate immunity [21]. During acute liver injury, infiltrating neutrophils produce ROS, secrete IL-1β, TNF-α and other pro-inflammatory cytokines, recruit inflammatory monocytes, promote liver inflammation and aggravate liver disease [22,23]. Macrophages are a key cellular component of the liver and play an important role in maintaining liver homeostasis as well as damage and repair in acute and chronic liver diseases. During liver injury, resident Kupfer cells sense homeostasis disturbances, interact with the hepatocyte population and release chemokines to recruit circulating white blood cells, including monocytes, which then differentiate into monocyt-derived macrophages in the liver [24,25].

In summary, it can be analyzed that aluminum is a substance with chronic toxic effects, which may lead to the occurrence of inflammation in the body, and it is related to the concentration and action time. The low-dose group has little influence on various white blood cells in the blood, and only under the continuous high concentration, the immune cells of the body can fully respond and produce immune response.

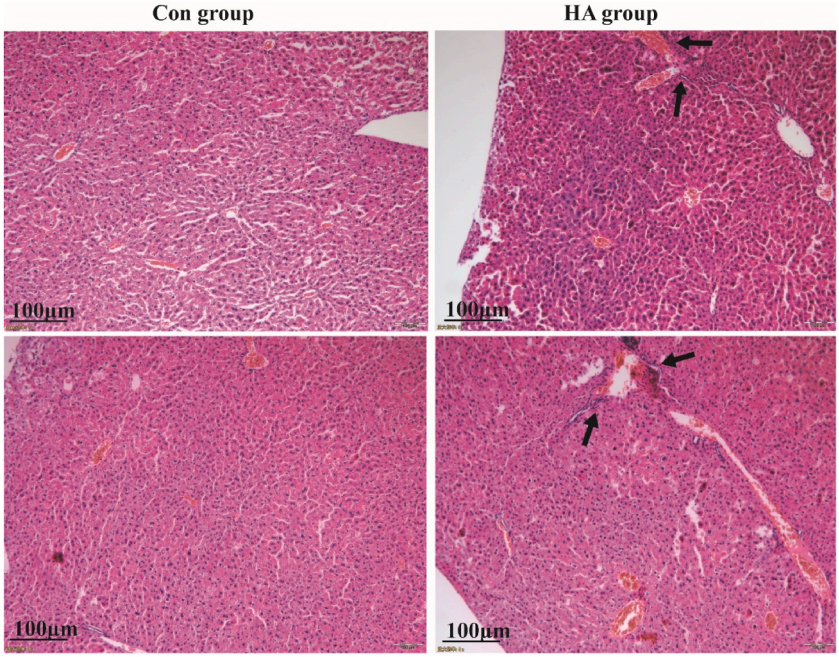

Fig. 2. HE staining section of mouse liver. The left and right column were brain tissue and liver slices from the control group and the HA group, respectively. The arrows show many gaps of different sizes in the cytoplasm, with the nuclei blurred and pushed to one side. It indicates the phenomenon of hepatic cell inflammation.

3.3. Histological observation

As shown in Fig. 2, in the liver sections of the HA group, more spaces of different sizes could be seen in the cytoplasm, and liver cells showed fatty inflammation and lesions. This indicates that the lipid metabolism of the liver may be abnormal, resulting in liver damage. No obvious abnormality was found in the tissue sections of LA group.

3.4. Effects on oxidative stress and liver function in mice

The effect of aluminum on MDA in liver is shown in Fig. 3A, in which MDA content in LA and HA groups was increased by 9.77 % and 31.52 %, respectively, compared with CON group, and the difference between HA group and CON group was significant ($P < 0.05$). MDA is a kind of lipid oxidation products which can reflects the degree of oxidation in the tissue, and the higher the content of MDA, the more serious the tissue oxidative damage. The experimental results show that with the increase of aluminum concentration, the degree of oxidation to liver tissue becomes higher and higher, in a concentration-dependent relationship. GSH-Px activity was shown in Fig. 3B. Compared with the control group, the activity of GSH-Px in group LA was significantly decreased by 20.34 % ($P < 0.001$) and that in group HA was significantly decreased by 21.85 % ($P < 0.001$), indicating that aluminum-induced oxidative damage

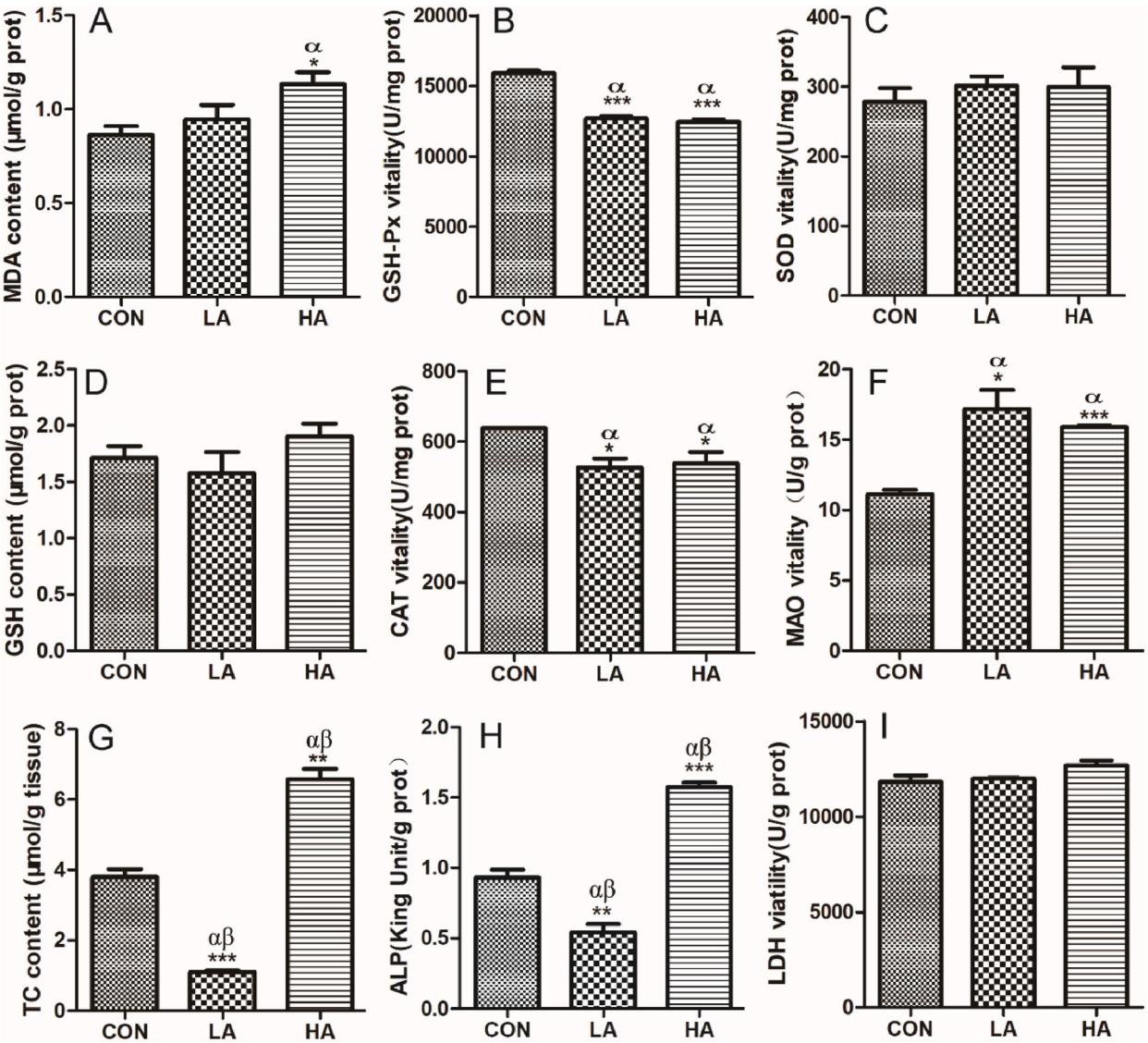

Fig. 3. Effects of aluminum on oxidative stress and liver function in mice. A-I are MDA、GSH-Px、SOD、GSH、CAT、MAO、TC、ALP and LDH, respectively. α index refers to the comparison of significant differences between the treatment group and the CON group, and β index refers to the comparison of significant differences between the treatment group. The error bars indicate S. E. M. n = 3. $^{*}P < 0.05$, $^{**}P < 0.01$, $^{***}P < 0.001$.

reduced the activity of GSH-Px. The effect of aluminum on CAT activity in liver tissue is shown in Fig. 3E. CAT activity in LA and HA groups decreased by 17.43 % and 15.54 %, respectively, with significant differences compared with the control group ($P < 0.05$), indicating that aluminum induced oxidative damage caused the decrease in CAT activity. There were no significant differences in GSH content and SOD activity among all groups (Fig. 3C–D), which may be due to the decrease in the activity of GSH-Px leading to the decrease in the ability to catalyze GSH, and aluminum is a chronic harmful substance, which has no obvious effect on the activity of some enzymes. CAT and GSH-Px are important antioxidant enzymes in the body, excessive free radicals and peroxides will lead to oxidative damage in cells and tissues, CAT can catalyze the decomposition of peroxides, while GSH-Px can remove free radicals and peroxides to reduce oxidative damage in the body, and the decrease of enzyme activity will reduce the antioxidant capacity of the body.

Some indexes of liver function were shown in Fig. 3F–I. Except for LDH, which had no significant difference among the groups, the other indexes of MAO, TC and ALP had significant changes among the groups. MAO is one of the indicators reflecting liver fibrosis and inflammatory diseases. Compared with the control group, the activity of MAO in LA and HA groups was significantly increased by 54.59 % ($P < 0.05$) and 43.08 % ($P < 0.001$), respectively, indicating that the liver was damaged to some extent with the increase of aluminum concentration. ALP is a metalloenzymes containing zinc, that is widely distributed in human liver, bone, intestine, kidney, placenta and other tissues, and is excreted from the liver to the bile. ALP in LA group was significantly decreased ($P < 0.01$). The possible reason is that aluminum ion can reduce the concentration of zinc ion [26], and occupy part of the protein binding site of zinc ion at low concentration, which affects the synthesis of ALP. ALP in HA group was significantly increased ($P < 0.001$), indicating that high concentration of aluminum may lead to liver inflammation and other diseases. The content of TC in HA group was significantly increased. This may be due to the fact that when the concentration of aluminum ions is relatively low, it interferes with the absorption of nutrients in the body, resulting in the reduction of cholesterol synthesis. The content of TC in HA group was significantly increased by 73.26 % ($P < 0.01$), indicating that aluminum had a certain effect on the interference of fat metabolism in liver. The study of Bhasin et al. [27] also reached a similar conclusion. The results of this study indicate that aluminum can cause oxidative stress in liver cells and abnormal liver function, which may further lead to liver tissue injury.

3.5. Effects of APS on the contents of TNF-α and IL-1β in mouse liver

As shown in Fig. 4, the TNF-α content in LA and HA groups was increased by 19.10 % ($P < 0.05$) and 16.92 %, respectively, compared with that in CON group. Compared with CON group, the increase in HA group was not statistically significant, which may be due to the fact that inflammation had already occurred at this time, leading to a decrease in the level of pro-inflammatory factors compared with LA group. IL-1β content in LA and HA groups was increased by 0.74 % and 5.45 %, respectively, compared with CON group, and there was no significant difference among groups. These results indicate that the pro-inflammatory factor TNF-α in liver tissue is more affected by aluminum than IL-1β, which is more likely to trigger cellular inflammatory response. TNF-α is the earliest and most important inflammatory mediator in inflammatory response. It can activate neutrophils and lymphocytes, increase cell permeability, regulate metabolic activities in other tissues, promote the synthesis and release of other cytokines, and play an important role in regulating development and immune processes, including inflammation, lipid metabolism and apoptosis. It is associated with various diseases [28]. The aforementioned neutrophils, along with the necrosis of neutrophils, as well as other cells such as monocytes and dendritic cells, can also activate the production of TNF-α in neighboring cells such as fibroblasts or macrophages [29]. This experiment indicated that aluminum might induce inflammation in hepatocytes and abnormal lipid metabolism, and the results were similar to the conclusions of El-Sayed et al. [30].

3.6. Changes of the structure and diversity of the gut microbiome community

According to the relative OTU abundance, LEfSe analysis could identify the characteristics of different abundance and associated categories. Kruskal-Wallis sum-rank test detected the species abundance differences among different groups, and obtained significantly different species biomarkers. Then Wilcoxon rank-sum test was used to test the difference consistency between different groups (between two groups) of the different species in the previous step. Results Cladogram was used to show the biomarker and its

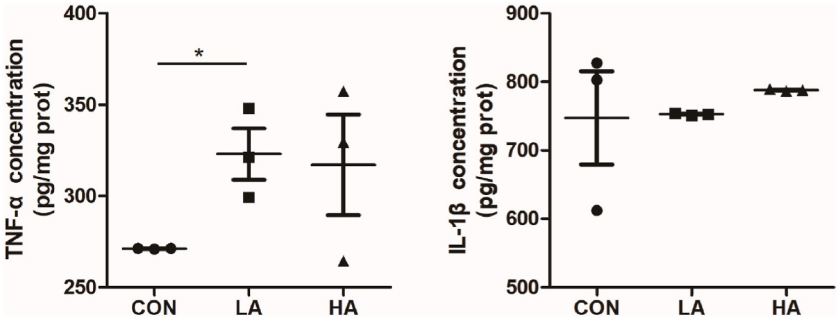

Fig. 4. Effects of aluminum on the contents of TNF-α and IL-1β in mouse liver tissue. The error bars indicate S. E. M. n = 3. *$P < 0.05$.

abundance at each taxonomic level (Fig. 5). Linear discriminant analysis (LDA) was used to estimate the influence of the abundance of each group (species) on the differential effect. The greater the LDA score (Fig. 6), the greater the influence of species abundance on the differential effect. The results showed that at phylum to genus level, there were 29, 34 and 40 communities or species in the normal group, LA group and HA group that had significant difference on sample division when LDA was greater than 2. When LDA is greater than 3, there are 23, 20 and 24, respectively. When the LDA is greater than 3.5, there are 9, 11, 11, respectively.

According to the Cladogram and LDA scores, the abundances of Firmicutes, Bacilli, Lactobacillales, *Lactobacteriaceae*, *Lactobacillus*, Staphylococcales, *Staphylococcaceae* and *Staphylococcus* in CON group varied greatly. The abundances of Actinobacteria (family), Bifidobacteriales (family and genus) and *Turicibacter* in HA group were significantly different in the same level. It is further indicated that these bacteria groups are the most affected species by the disturbance of aluminum, and they are also the key targets for the subsequent effects on the organism. The accuracy of species screening for significant differences in our previous research results was verified [31]. The gut microbiota affects liver lipid metabolism through the gut-liver axis, and perturbations of the gut microbiota, such as antibiotics, impair the production of bacterial metabolites, which are typically components of liver cell membrane lipids. Gut microbiota is the key to liver regeneration and liver membrane phospholipid biosynthesis [32]. Intestinal flora is involved in the regulation of the immune microenvironment of the liver, thereby regulating the release of inflammatory factors such as HGF, IL-6, TNF-α, IFN-γ and TGF-β, which are involved in different stages of liver regeneration [33]. Dysregulation of the gut microbiota has been identified in liver diseases of various etiologies, including viral hepatitis, acute liver injury, non-alcoholic fatty liver disease, alcohol-related liver disease, primary cholangitis, primary sclerosing cholangitis, and autoimmune hepatitis [34,35].

By comparison, PICRUSt predicted 42 pathways at the level-2 level in KEGG functional annotation, and the pathways with high abundance were: carbohydrate metabolism, amino acid metabolism, membrane transport, lipid metabolism, biosynthesis,

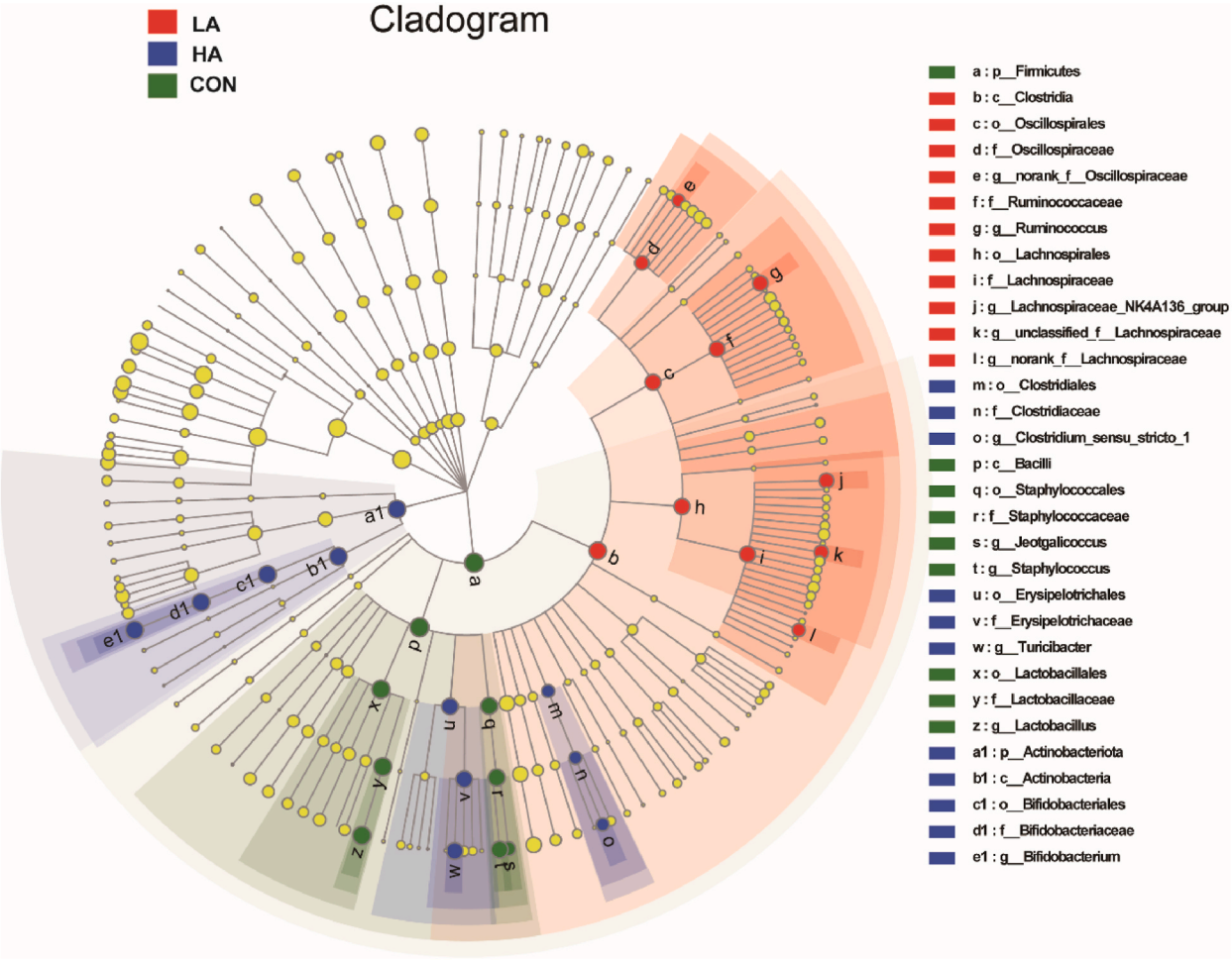

Fig. 5. Cladogram of LEfSe multilevel species hierarchy. Different circles radiate from inside to outside representing seven taxonomic levels of phylum compendium. The light-yellow nodes indicate that there is no significant difference between groups. Other nodes with different colors represent microbial groups that are significantly enriched in the corresponding groups and have a significant effect on the differences between groups. The higher the abundance, the larger the nodes. (For interpretation of the references to color in this figure legend, the reader is referred to the Web version of this article.)

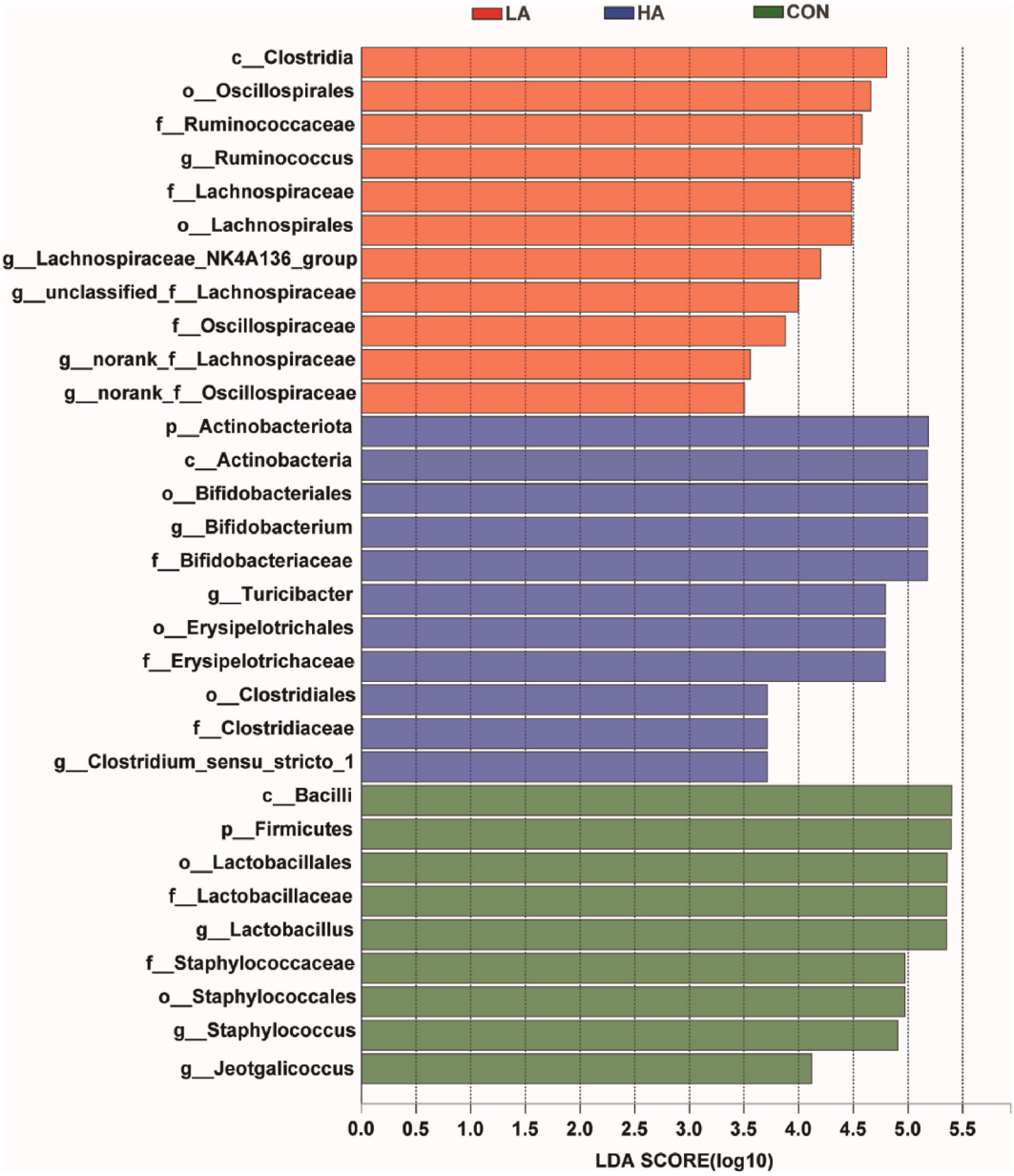

Fig. 6. LDA discriminant histogram; The abscissa is the LDA score, and the ordinate is the microbial group whose abundance has a significant effect on the difference.

biodegradation and metabolism of other secondary metabolites, etc. All samples were screened at the level of level 3 and 268 KEGG pathways were predicted (Fig. 7). Pathways with high microbial abundance in each sample included metabolic pathways, secondary metabolites synthesis, microbial metabolism in different environments, amino acid synthesis, ABC transporters, carbon metabolism, etc. Through the prediction, the direction is provided for the verification of subsequent experiments. Microbial-derived gut metabolites are key contributors to host phenotypes, many of which can link microbiome composition to metabolic diseases [36]. Le et al. employed a labeling strategy to trace and characterize bacterial sphingolipids from the intestinal symbiont *Bacteroides thetaiotaomicron* to the liver and colon of mice. Bacterial sphingolipid synthesis was found to alleviate excess lipid accumulation in a mouse model of hepatic steatosis, and previously uncharacterized bacterial sphingolipid transport to the liver was observed [37].

Using microbiome BugBase tools (https://bugbase.cs.umn.edu/index.html), to determine the microbial groups of samples in high level phenotype, phenotypic prediction and significant difference analysis (Fig. 8). Phenotypes include Gram Positive, Gram Negative, Forms Biofilms, Contains Mobile Elements, aerobic, anaerobic and Stress Tolerant. It can be seen from the figure that the abundance of oxidation stress tolerance type is the highest, which reveals that the oxidative stress induced by aluminum induces the increase of the abundance of oxidation tolerance type in microorganisms.

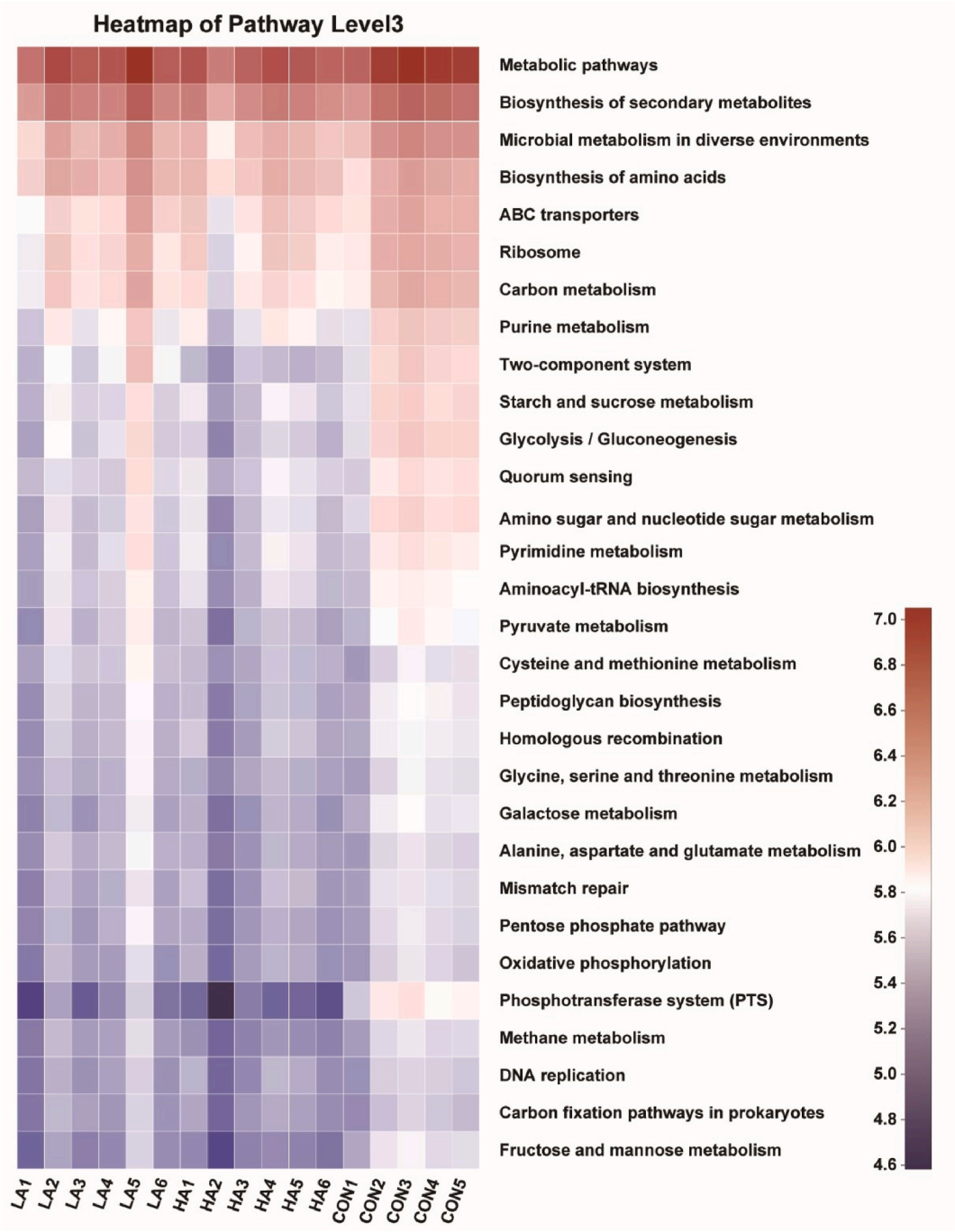

Fig. 7. Heatmap of KEEG Pathway Level 3 (top 30). Abscissa is the predicted path name, and the ordinate represents the predicted pathway. Color indicates abundance, and the redder the color, the higher the abundance. (For interpretation of the references to color in this figure legend, the reader is referred to the Web version of this article.)

4. Conclusion

This study revealed that an increase in aluminum content resulted in a suppression of body weight growth and significant alterations in the composition of white blood cells. Histological examination demonstrated liver lesions and inflammation through HE staining. Notably, oxidative stress markers indicated a substantial rise in MDA levels, while GSH-PX and CAT levels significantly decreased in the aluminum-treated group, indicating oxidative damage to the tissue. Liver function indexes MAO, TC, and ALP exhibited significant changes across all groups, indicating oxidative stress-induced liver cell dysfunction. Pro-inflammatory factor

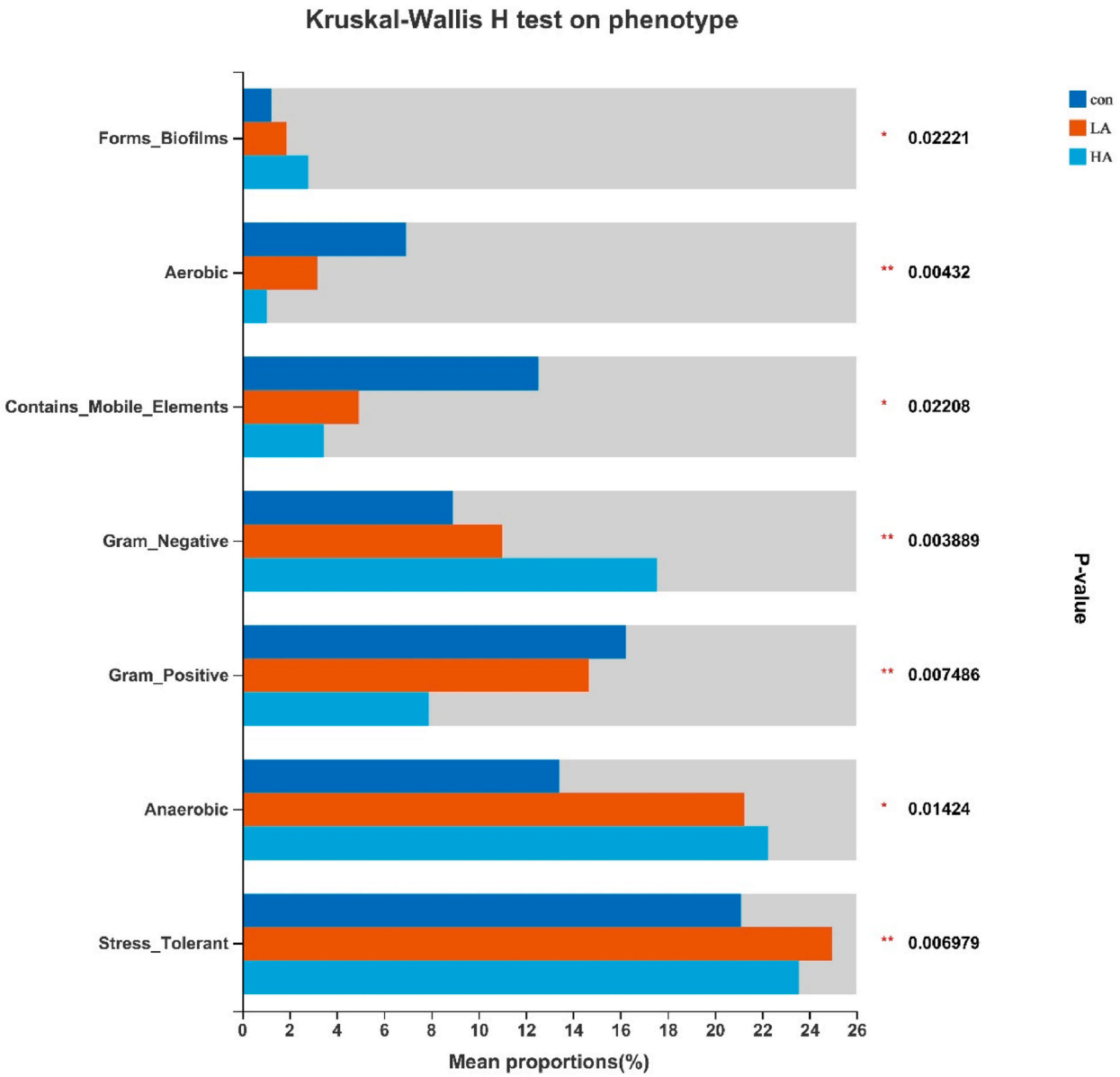

Fig. 8. Phenotypic differences among CON, LA and HA groups; The ordinate indicates the name of the phenotype, the abscissa indicates the percentage value of the relative abundance of the phenotype.

TNF-α displayed notable variations as well. Furthermore, exposure to Al led to significant modifications in the structure of intestinal flora, particularly affecting microbial species with higher relative abundance changes which became the primary focus for future investigations. Predictions regarding microbial phenotypes suggested that aluminum-induced oxidative stress promoted an increase in oxidation-tolerant microorganisms' abundance. Alterations within gut flora structure also influenced liver health via the gut-liver axis. These findings provide a theoretical foundation for exploring inflammatory microbial intervention markers and metabolic pathways aimed at reducing aluminum toxicity; moreover, identifying relevant microbial species exhibiting significant differences remains crucial for subsequent studies. There are also many shortcomings in this study, such as whether liver deficiency causes changes in gut microbiota and their bidirectional regulatory effects. This will be our next research direction: the demonstration of causality.

Data availability statement

The datasets presented in this study can be found in online repositories. The names of the repository/repositories and accession number(s) can be found below: NCBI, Submission ID: SUB11009633、11062312, BioProject ID: PRJNA804675、805015.

CRediT authorship contribution statement

Rong Feng: Writing – original draft, Project administration, Methodology, Investigation. **Liang Chen:** Writing – review & editing, Software, Formal analysis. **Ming Yang:** Writing – original draft, Data curation.

Declaration of competing interest

The authors declare again that they have no known competing financial interests or personal relationships that could have appeared to influence the work reported in this paper.

Acknowledgements

This research did not receive any specific grant from funding agencies in the public, commercial, or not-for-profit sectors.

References

[1] M.J. Balgoon, Assessment of the protective effect of lepidium sativum against aluminum-induced liver and kidney effects in albino rat, BioMed Res. Int. 2019 (2019) 4516730.
[2] S.M. Galal, H.F. Hasan, M.K. Abdel-Rafei, S.M. El Kiki, Synergistic effect of cranberry extract and losartan against aluminium chloride-induced hepatorenal damage associated cardiomyopathy in rats, Arch. Physiol. Biochem. 125 (2019) 357–366.
[3] M. Al-Kahtani, M.M. Abdel-Daim, A.A. Sayed, A. El-Kott, K. Morsy, Curcumin phytosome modulates aluminum-induced hepatotoxicity via regulation of antioxidant, Bcl-2, and caspase-3 in rats, Environ. Sci. Pollut. Res. Int. 27 (2020) 21977–21985.
[4] S.J. Mandriota, et al., Genomic instability is an early event in aluminium-induced tumorigenesis, Int. J. Mol. Sci. 21 (2020) 9332.
[5] R. Feng, L. Chen, K. Chen, Cytotoxicity and changes in gene expression under aluminium potassium sulfate on Spodoptera frugiperda 9 cells, Ecotoxicology 30 (2021) 2056–2070.
[6] I. Said, H. Ahad, A. Said, Gut microbiome in non-alcoholic fatty liver disease associated hepatocellular carcinoma: current knowledge and potential for therapeutics, World J. Gastrointest. Oncol. 14 (2022) 947–958.
[7] R.S. Lin, et al., Endotoxemia in patients with chronic liver diseases: relationship to severity of liver diseases, presence of esophageal varices, and hyperdynamic circulation, J. Hepatol. 22 (1995) 165–172.
[8] K. Guo, S. Xu, Z. Zeng, "Liver–gut" axis: a target of traditional Chinese medicine for the treatment of non-alcoholic fatty liver disease, Front. Endocrinol. 13 (2022) 1050709.
[9] D. Cheng, C. Zhu, J. Cao, W. Jiang, The protective effects of polyphenols from jujube peel (Ziziphus Jujube Mill) on isoproterenol-induced myocardial ischemia and aluminum-induced oxidative damage in rats, Food Chem. Toxicol. 50 (2012) 1302–1308.
[10] R.A. Abdel-Aal, A.A.A. Assi, B.B. Kostandy, Rivastigmine reverses aluminum-induced behavioral changes in rats, Eur. J. Pharmacol. 659 (2011) 169–176.
[11] Pauluhn Jürgen, Pulmonary toxicity and fate of agglomerated 10 and 40 nm aluminum oxyhydroxides following 4-week inhalation exposure of rats: toxic effects are determined by agglomerated, not primary particle size, Toxicological Sciences An Official Journal of the Society of Toxicology 152 (2009), https://doi.org/10.1093/toxsci/kfp046.
[12] B. Amulic, C. Cazalet, G.L. Hayes, K.D. Metzler, A. Zychlinsky, Neutrophil function: from mechanisms to disease, Annu. Rev. Immunol. 30 (2012) 459–489.
[13] T.E. Decoursey, E. Ligeti, Regulation and termination of NADPH oxidase activity, Cell. Mol. Life Sci. 62 (2005) 2173–2193.
[14] P. Nunes, N. Demaurex, M.C. Dinauer, Regulation of the NADPH oxidase and associated ion fluxes during phagocytosis, Traffic 14 (2013) 1118–1131.
[15] R. Teschke, Aluminum, arsenic, beryllium, cadmium, chromium, cobalt, copper, iron, lead, mercury, molybdenum, nickel, platinum, thallium, titanium, vanadium, and zinc: molecular aspects in experimental liver injury, Int. J. Mol. Sci. 23 (2022) 12213.
[16] M.R. Rahimzadeh, et al., Aluminum poisoning with emphasis on its mechanism and treatment of intoxication, Emerg Med Int 2022 (2022) 1480553.
[17] C. Kaltenmeier, et al., The role of neutrophils as a driver in hepatic ischemia-reperfusion injury and cancer growth, Front. Immunol. 13 (2022) 887565.
[18] A. Banasik, A. Lankoff, A. Piskulak, K. Adamowska, A. Wojcik, Aluminum-induced micronuclei and apoptosis in human peripheral-blood lymphocytes treated during different phases of the cell cycle, Environ. Toxicol. 20 (2010) 402–406.
[19] Nazareth Fernandes Paz Letícia, Mesquita Moura Laís, D.C.A. Feio, M.D.S.G. Cardoso, Patrícia Danielle L. Lima, Corrigendum to 'Evaluation of in vivo and in vitro toxicological and genotoxic potential of aluminum chloride' [Chemosphere 175 (2017), 130–137], Chemosphere 193 (2017) 1244–1245.
[20] A. Lankoff, et al., A comet assay study reveals that aluminium induces DNA damage and inhibits the repair of radiation-induced lesions in human peripheral blood lymphocytes, Toxicol. Lett. 161 (2006) 27–36.
[21] H. Vrieling, S. Kooijman, J.W.D. Ridder, D.M.E. Thies-Weesie, B. Metz, Activation of human monocytes by colloidal aluminum salts, J. Pharmaceut. Sci. 109 (2019).
[22] F. Heymann, F. Tacke, Immunology in the liver–from homeostasis to disease, Nat. Rev. Gastroenterol. Hepatol. 13 (2016) 88–110.
[23] R. Xu, H. Huang, Z. Zhang, F.-S. Wang, The role of neutrophils in the development of liver diseases, Cell. Mol. Immunol. 11 (2014) 224–231.
[24] O. Krenkel, F. Tacke, Liver macrophages in tissue homeostasis and disease, Nat. Rev. Immunol. 17 (2017) 306–321.
[25] Y. Wen, J. Lambrecht, C. Ju, F. Tacke, Hepatic macrophages in liver homeostasis and diseases-diversity, plasticity and therapeutic opportunities, Cell. Mol. Immunol. 18 (2021) 45–56.
[26] Y. Zhu, et al., Effects of aluminum trichloride on the trace elements and cytokines in the spleen of rats, Food Chem. Toxicol. 50 (2012) 2911–2915.
[27] P. Bhasin, N. Singla, D.K. Dhawan, Protective role of zinc during aluminum-induced hepatotoxicity, Environ. Toxicol. 29 (3–4) (2014) 320–327.
[28] D. Keith, L. Ying, S. Gary, Adiponectin action: a combination of endocrine and autocrine/paracrine effects, Front. Endocrinol. 2 (2011) 62.
[29] M. Li, et al., An essential role of the NF-kappa B/Toll-like receptor pathway in induction of inflammatory and tissue-repair gene expression by necrotic cells, J. Immunol. 166 (2001) 7128–7135.
[30] E.S.A. B, A.K. A, A.M.A. C, Prophylactic and therapeutic effects of taurine against aluminum-induced acute hepatotoxicity in mice, J. Hazard Mater. 192 (2011) 880–886.
[31] R. Feng, et al., Based on 16 S rRNA sequencing and metabonomics to reveal the new mechanism of aluminum potassium sulfate induced inflammation and abnormal lipid metabolism in mice, Ecotoxicol. Environ. Saf. 247 (2022) 114214.
[32] Y. Yin, et al., Gut microbiota promote liver regeneration through hepatic membrane phospholipid biosynthesis, J. Hepatol. 78 (2023) 820–835.
[33] Z. Xu, N. Jiang, Y. Xiao, K. Yuan, Z. Wang, The role of gut microbiota in liver regeneration, Front. Immunol. 13 (2022) 1003376.
[34] J.S. Bajaj, A. Khoruts, Microbiota changes and intestinal microbiota transplantation in liver diseases and cirrhosis, J. Hepatol. 72 (2020) 1003–1027.
[35] D. Tokuhara, Role of the gut microbiota in regulating non-alcoholic fatty liver disease in children and adolescents, Front. Nutr. 8 (2021) 700058.
[36] K.A. Krautkramer, J. Fan, F. Bäckhed, Gut microbial metabolites as multi-kingdom intermediates, Nat. Rev. Microbiol. 19 (2021) 77–94.
[37] H.H. Le, M.-T. Lee, K.R. Besler, E.L. Johnson, Host hepatic metabolism is modulated by gut microbiota–derived sphingolipids, Cell Host Microbe 30 (2022) 798–808.e7.